

Spin polarization at Fe/Cr interfaces

L. Pizzagalli, M. Freyss, G. Moraitis, D. Stoeffler, C. Demangeat, and H. Dreysse
IPCMS-GEMME, 67037 Strasbourg, France

A. Vega

Departamento de Física Teórica, Universidad de Valladolid, 47011 Valladolid, Spain

S. Miethaner and G. Bayreuther

Institut für Angewandte Physik, Universität Regensburg, 93040 Regensburg, Germany

It is shown that contradictory experimental data on magnetic moments and spin order at Fe/Cr interfaces can be explained by structural irregularities at the interfaces. The spin-polarized electronic charge distribution was calculated by using a self-consistent tight-binding model combined with a real-space recursion method. It was used to interpret the total magnetic moment of Cr(001) films and of Cr/Fe(001) sandwiches molecular beam epitaxy grown on Fe(001) from *in situ* measurements with an alternating gradient magnetometer during film growth. While a strong decrease of the sample moment during Cr deposition was observed on a very smooth surface, no moment change occurred for a strongly faceted surface. The different results of both experiments are consistent with the calculations if we take into account (i) a possible ferrimagnetic $c(2 \times 2)$ spin configuration of a Cr monolayer on Fe(001) which might be favorable in clusters of a certain size and for high step densities; (ii) a possible interchange of one Cr and Fe monolayer at the interface; and (iii) a multidomain configuration with zero net moment of a thin Fe layer on a Cr surface due to a high step density. © 1997 American Institute of Physics. [S0021-8979(97)45808-5]

I. INTRODUCTION

Tight-binding calculations by Victora and Falicov¹ and the full-potential linearized-augmented-plane-wave (FLAPW) results of Fu and Freeman² predicted strongly enhanced magnetic moments of more than $3 \mu_B$ for one monolayer of Cr deposited on an ideal Fe(001) surface as well as an antiparallel orientation of the Cr and Fe moments. However, many experiments (e.g., by photoelectron spectroscopy³ or x-ray circular dichroism⁴) did not succeed in verifying this prediction. Recently, by using an *in situ* alternating gradient magnetometer (AGM), it was possible to observe Cr moments up to $4 \mu_B$ for submonolayer Cr on Fe(001) and an average moment of $3 \mu_B$ for a 1 ML Cr film.⁵ In addition, in agreement with theory, it was found that the first Cr monolayer couples antiferromagnetically to the Fe magnetization and that there is a significant deviation from layer-antiferromagnetic order in the first few monolayers of thicker Cr films on Fe(001).

Up to recently the theoretical predictions were based on ideal surfaces and interfaces, whereas structural defects (steps, vacancies, interdiffusion etc.) are known to occur in the growth process. Due to the antiferromagnetic coupling between Fe and Cr, structural defects at the interface may be expected to create an interesting variety of magnetic behaviors. The results presented here give compelling evidence that the presence of such defects at the surfaces of the substrates is the origin of some of the curious magnetic behavior experimentally observed earlier, e.g., a zero net magnetic moment of a Cr layer grown on a stepped Fe surface.⁶ It will be shown below how some of these discrepancies in the experimental findings may be traced back to structural irregularities at the interfaces.

II. THEORY

The spin-polarized electronic charge distribution was calculated by using a self-consistent tight-binding model in combination with a recursion method in the real space.^{7,8} For this model, two essential parameters are used: $\beta(i,j)$, the hopping integrals between sites i and j obtained in the canonical description from the width of the d bands and J_i ($i = \text{Cr, Fe}$) for the exchange parameter adjusted in order to recover the experimental magnetic moments for Cr and Fe, i.e., $0.6 \mu_B$ for Cr and $2.2 \mu_B$ for Fe. At the interface, we assume

$$\beta(\text{FeCr}) = \sqrt{\beta(\text{FeFe}) \cdot \beta(\text{CrCr})}.$$

These model calculations have given, in the case of periodic systems, like Fe/Cr superlattices or Fe/Cr/Fe sandwiches,^{9,10} satisfactory agreement with methods using the local-density approximation (LDA).¹¹ However, even the best LDA calculations yield the wrong ground state for Fe (fcc phase).¹² Only after improving the exchange correlation by adding gradient correction to the exchange-correlation energy the ground state of the Fe crystal is found to be indeed bcc.¹³ Chen *et al.*¹⁴ have shown, using LDA, that the ground state of bulk Cr is nonmagnetic. They interpret this failure as an indication that LDA does not adequately describe Cr and that it may be necessary to go beyond the LDA to perform reliable calculations of structural and magnetic properties of bulk Cr and its surfaces and interfaces.

Moraitis *et al.*¹⁵ have recently performed calculations on Fe_1Cr_m superlattices ($m = 1, \dots, 7$) using TB-LMTO code with LDA. The calculation displays, for the ground state, parallel alignment of Fe and Cr spins at the Fe/Cr interfaces as compared to antiparallel configuration in the case of Fe_2Cr_m superlattices.¹¹ However, when the lattice parameter is increased, a spin flip occurs between Fe and Cr in Fe_1Cr_m

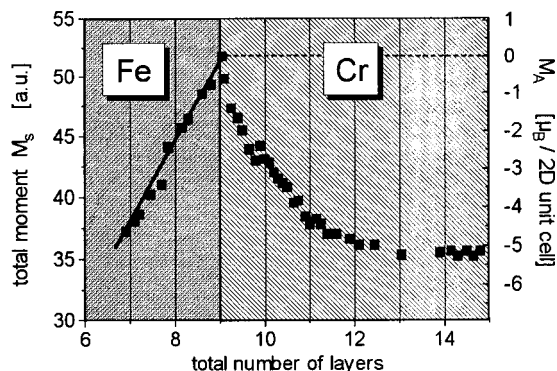


FIG. 1. Spontaneous magnetic moment of a film grown on Au(001) during sequential deposition of Fe(001) and Cr(001). The scale at the right side gives the areal density of the moment change during Cr deposition, i.e., the integral moment change normalized to the number of atoms in the surface (data from Ref. 5).

superlattices.¹⁵ Moreover, LDA leads to a 3-layer period of the interlayer exchange coupling.¹⁵ This last result should be considered as an “artifact” of the LDA approximation. The general gradient approximation (GGA) of Perdew and Wang¹⁶ leads to very different results for Fe_1Cr_m superlattices:

- (1) the relative orientation of Fe and Cr spins in the interface layers oscillates between parallel and antiparallel versus m ; and
- (2) a 2-layer period is now recovered for the interlayer exchange coupling.

III. EXPERIMENT

Fe(001) films and Fe/Cr(001) sandwiches were epitaxially grown in UHV ($p \approx 2 \times 10^{-10}$ mbar) on Au(001) films which in turn were grown on LiF(001) substrates. The film structure was verified by low-energy electron diffraction (LEED) and *ex situ* by transmission electron microscopy and diffraction. The magnetic moment of the samples was continuously measured *in situ* during growth using an alternating gradient magnetometer (AGM) in magnetic fields up to 9 kOe.

In a first experiment,⁵ the deposition of a Cr layer on a flat Fe film was accompanied by a drastic reduction of the sample moment as shown in Fig. 1. This behavior was explained by assuming a random growth of the Cr layer, antiferromagnetic coupling between Fe and Cr moments at the interface, and large Cr surface and interface moments.⁵ In a second experiment⁶ by using particular growth conditions (e.g., growth temperature 300 K) and after depositing several Au/Fe/Cr sandwich layers, strongly faceted surfaces resulted with a large step density. After the deposition of a gold layer of 30 Å, a Fe film of 12.6 Å was deposited followed by 8.4 Å of Cr, 12.2 Å of Fe, and a further Au layer (all grown at 300 K). The spontaneous magnetic moment as obtained from extrapolating the magnetization curves from fields between 1 and 2 kOe to $H=0$ is shown in Fig. 2 for this deposition sequence. We observe that the magnetic moment of the sample does not change upon deposition of Cr on top of the

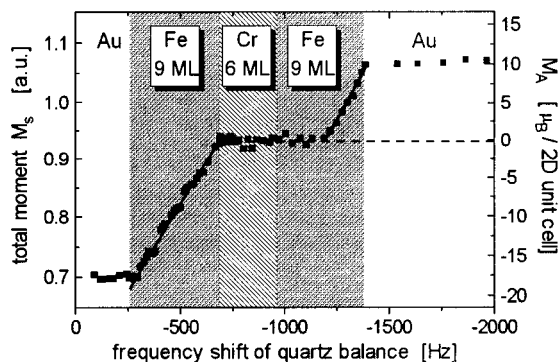


FIG. 2. Spontaneous magnetic moment of a film grown on a faceted Au(001) film with underlying Fe/Cr layers during deposition of a Fe/Cr/Fe sandwich film (scale as in Fig. 1). The thicknesses were verified *ex situ* by x-ray fluorescence spectroscopy (data from Ref. 6).

first Fe film in contrast to the first experiment. Furthermore, the moment of a second Fe layer remains practically zero up to about 5 monolayer (ML).

IV. DISCUSSION

The two experiments presented in Sec. III differ in various aspects and are in some way representative of other results reported previously. It will be shown in this section that apparent discrepancies can in principle be understood as a consequence of different structural details of the samples under investigation. The discussion will concentrate on three different phenomena: (i) the net magnetic moment of the submonolayer Cr films grown on Fe(001); (ii) the total magnetic moment of thickened Cr films of Fe(001); (iii) the net moment of a second Fe layer grown on top of Cr/Fe(001).

A. Submonolayer Cr on Fe(001)

The average moment of a submonolayer Cr film on Fe is determined from the initial slope of the total sample moment versus Cr thickness. From the first experiment⁵ (see Fig. 1), we deduce a value of $\mu_{Cr} \approx 4 \mu_B$, from the second experiment⁶ (Fig. 2), we find $\mu_{Cr} \approx 0$. It has been shown earlier⁶ that the last result is not related to contamination. These different results can be explained as follows: Vega *et al.*¹⁷ have investigated the possibility of a ferrimagnetic-in-plane configuration with $c(2 \times 2)$ symmetry for Cr monolayer on Fe(001) (see Fig. 3). The difference of total energy with the well established $p(1 \times 1)^{-}$ (in-plane ferromagnetic coupling in the Cr overlayer combined with antiparallel alignment between Cr and Fe moments) is less than 1 mRy. Therefore, either the $c(2 \times 2)$ configuration with nearly zero net moment or $p(1 \times 1)^{-}$ with large negative net moment can be expected in the experiments. We therefore could understand our experiments if we assume that in a Cr film grown on a faceted Fe surface⁶ the $c(2 \times 2)$ configuration is formed whereas the $p(1 \times 1)^{-}$ configuration is present in the earlier experiment⁵ and is responsible for the large negative slope of the magnetic moment at the beginning of the growth of Cr on Fe(001). Moreover, it has been shown¹⁸ that small clusters of Cr on flat Fe(001) surfaces favor the $p(1 \times 1)^{-}$ configuration whereas bigger ones lead to $c(2 \times 2)$. Future *in situ* observa-

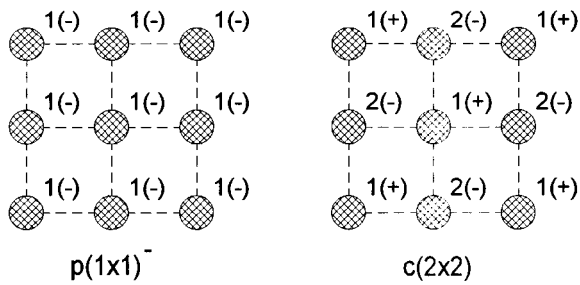


FIG. 3. Two different spin configurations for one monolayer of Cr on an Fe(001) surface: $p(1\times 1)^-$ configuration with in-plane ferromagnetic order of Cr moments in antiparallel alignment relative to the Fe moments compared to a $c(2\times 2)$ ferrimagnetic configuration. (+) and (-) indicate the spin orientation relative to the Fe spins (+) of the substrate (from Ref. 19).

tions of the cluster size with scanning tunneling microscope (STM) should allow to check this interpretation. Furthermore, the $c(2\times 2)$ configuration can minimize frustration at step edges and therefore be the preferred one for high step densities (see Sec. IV B)

B. Thick Cr layers

A large total moment change of $\approx -5 \mu_B$ per 2D unit cell was observed for thick Cr layers in the first experiment (Fig. 1). Stoeffler *et al.*¹⁹ have shown that this large moment reduction can be reproduced in a physically meaningful model if an interchange of one Cr and Fe monolayer is assumed to occur at the interface after deposition of the second Cr monolayer. Of course, a nonlayer-by-layer growth needs to be included in the model in order to kill the oscillations in the magnetic profiles versus Cr deposition. A natural interdiffusion at the Fe/Cr interface has indeed been verified recently by STM and tunneling spectroscopy,²⁰ by ion surface scattering,²¹ and by angle-resolved Auger electron spectroscopy;²² however, a complete interchange between one Fe and one Cr layer has not been confirmed yet. The particular chemical order at the interface and the role of growth conditions remain to be elucidated.

In the second experiment, the total moment of Cr layer grown on a faceted Fe(001) surface remained practically zero (Fig. 2). This could simply mean that the $c(2\times 2)$ spin configuration persists once it has been formed in the early stage of growth. However, another mechanism could play a role: Stoeffler and Gautier⁸ have proposed to link the nearly zero moment to the presence of steps at the surface of Fe(001). In this case, a multiple domain configuration results (see Fig. 13 of Ref. 8) which leads to a very small total magnetic moment change when one Cr monolayer is added. This effect could also be of relevance for the formation of the $c(2\times 2)$ spin configuration discussed above because the ferrimagnetic state naturally reduces frustration at the step edges. To test the role of atomic steps, STM studies in combination with RHEED and *in situ* AGM measurements are under way.

C. Moment of Fe on Cr(001)

From Fig. 2, it is evident that a Fe layer deposited on a strongly stepped Cr surface does not have a net magnetic

moment up to 5 ML thickness. This effect must be a consequence of the particular Cr surface because the ferromagnetic order of the previous Fe layer grown on Au(001) is developed as expected.⁶

This behavior can be explained by irregularities at the surface of Cr(001) Vega *et al.*²³ have discussed the effect of prominences, steps, and valleys at the surface of Cr(001) on the magnetic map of Fe overlayers. Arising from a magnetic multidomain arrangement, a zero total magnetic moment is obtained when starting the Fe deposition in qualitative agreement with the experimental data of Fig. 2. Zero magnetic moment is obtained up to 4 ML of Fe in the case of small terrace width.

This interpretation is supported by the experimental observation that the critical thickness for the appearance of a ferromagnetic moment in the Fe layer varies for different samples. It is clearly necessary to determine the precise morphology of the surface by STM in order to allow a more quantitative comparison with the experiment, in particular, concerning the spin configuration close to the interface for larger Fe thicknesses.

ACKNOWLEDGMENTS

Support by D. Stoeffler, C. Demangeat, H. Dreyssé, S. Miethar, and G. Bayreuther of PROCOPE/DAAD and S. Miethaner and G. Bayreuther Deutsche Forschungsgemeinschaft is gratefully acknowledged.

¹R. H. Victora and L. M. Falicov, Phys. Rev. B **31**, 7335 (1985).

²C. L. Fu and A. J. Freeman, Phys. Rev. B **33**, 1755 (1986).

³F. U. Hillebrecht, Ch. Roth, R. Jungblut, E. Kisker, and A. Bringer, Europhys. Lett. **19**, 711 (1992).

⁴Y. U. Idzerda, L. H. Tjeng, H.-J. Lin, G. Meigs, C. T. Chen, and J. Gutierrez, J. Appl. Phys. **73**, 6204 (1993).

⁵C. Turtur and G. Bayreuther, Phys. Rev. Lett. **72**, 1557 (1994).

⁶S. Miethaner and G. Bayreuther, J. Magn. Magn. Mater. **148**, 42 (1995).

⁷A. Vega, C. Demangeat, H. Dreyse, and A. Chouairi, Phys. Rev. B **51**, 11 546 (1995).

⁸D. Stoeffler and F. Gautier, J. Magn. Magn. Mater. **147**, 260 (1995).

⁹D. Stoeffler and F. Gautier, Prog. Theor. Phys. Suppl. **101**, 139 (1990).

¹⁰A. Vega *et al.*, J. Appl. Phys. **69**, 4544 (1991).

¹¹F. Herman, J. Sticht, and M. Van Schilfgaarde, J. Appl. Phys. **69**, 4783 (1991).

¹²C. S. Wang, B. M. Klein, and H. Krakauer, Phys. Rev. Lett. **54**, 1852 (1985).

¹³D. Singh, D. Clougherty, J. MacLachen, R. C. Albers, and C. Wang, Phys. Rev. B **44**, 7701 (1991); D. Singh, W. Pickett, and H. Krakauer, *ibid.* **43**, 11 628 (1991).

¹⁴J. Chen, D. Singh, and H. Krakauer, Phys. Rev. B **38**, 12 834 (1988).

¹⁵G. Moraitis, M. A. Khan, C. Demangeat, and H. Dreyse, J. Magn. Magn. Mater. **156**, 250 (1996).

¹⁶Y. Wang and J.-P. Perdew, Phys. Rev. B **43**, 8911 (1991).

¹⁷A. Vega, S. Bouarab, H. Dreyse, and C. Demangeat, Thin Solid Films **275**, 103 (1996).

¹⁸L. Pizzagalli *et al.*, J. Appl. Phys. **79**, 5834 (1996).

¹⁹D. Stoeffler, A. Vega, H. Dreyse, and C. Demangeat, Mater. Res. Soc. Symp. Proc. **384**, 247 (1995).

²⁰A. Davis, J. A. Stroscio, D. T. Pierce, and R. J. Celotta, Phys. Rev. Lett. **76**, 4175 (1996).

²¹R. Pfandzelter, T. Igel, and H. Winter, Phys. Rev. B **54**, 4496 (1996).

²²D. Venus and B. Heinrich, Phys. Rev. B **53**, 1733 (1996).

²³A. Vega, D. Stoeffler, H. Dreyse, and C. Demangeat, Europhys. Lett. **31**, 561 (1995).